Bioconjugate Chemistry

Article

pubs.acs.org/bc

Synthesis and Transfection Efficiency of Cationic Oligopeptide Lipids: Role of Linker

Vijaya Gopal,[†] Jennifer Xavier,[†] Md. Zahid Kamal,[†] Srinath Govindarajan,[†] Makoto Takafuji,[‡] Shuta Soga,[‡] Takayuki Ueno,[‡] Hirotaka Ihara,[‡] and Nalam M. Rao*,[†]

[†]Centre for Cellular and Molecular Biology (Council of Scientific and Industrial Research), Uppal Road, Hyderabad, India 500007

[‡]Department of Applied Chemistry and Biochemistry, Kumamoto University, Kumamoto, Japan

Supporting Information

ABSTRACT: In the design of new cationic lipids for gene transfection, the chemistry of linkers is widely investigated from the viewpoint of biodegradation and less from their contribution to the biophysical properties. We synthesized two dodecyl lipids with glutamide as the backbone and two lysines to provide the cationic headgroup. Lipid 1 differs from Lipid 2 by the presence of an amide linkage instead of an ester linkage that characterizes Lipid 2. The transfection efficiency of lipoplexes with cholesterol as colipid was found to be very high with Lipid 1 on Chinese Hamster Ovary (CHO) and HepG2 cell lines, whereas Lipid 2 has shown partial transfection efficiency on HepG2 cells. Lipid 1 was found to be stable in the presence of serum when tested in HepG2 and CHO cells albeit with lower activity. Fluorescence-based dye-binding and agarose gel-based assays indicated that Lipid 1 binds to DNA more efficiently than Lipid 2 at charge ratios of >1:1. The uptake of oligonucleotides with Lipid 1 was higher than Lipid 2 as revealed by confocal microscopy. Transmission electron microscopy (TEM) images reveal distinct formation of liposomes and lipoplexes with Lipid 1 but fragmented and unordered structures with Lipid 2. Fusion of Lipids 1 and 2 with anionic vesicles, with composition similar to plasma membrane, suggests that fusion of Lipid 2 was very rapid and unlike a fusion event, whereas the fusion kinetics of Lipid 1 vesicles was more defined. Differential scanning calorimetry (DSC) revealed a high T_m for Lipid 1 (65.4 °C) while Lipid 2 had a T_m of 23.5 °C. Surface area–pressure isotherms of Lipid 1 was less compressible compared to Lipid 2. However, microviscosity measured using 1,6-diphenyl-1,3,5-hexatriene (DPH) revealed identical values for vesicles made with either of the lipids. The presence of amide linker apparently resulted in stable vesicle formation, higher melting temperature, and low compressibility, while retaining the membrane fluid properties suggesting that the intermolecular hydrogen bonds of Lipid 1 yielded stable lipoplexes of high transfection efficiency.

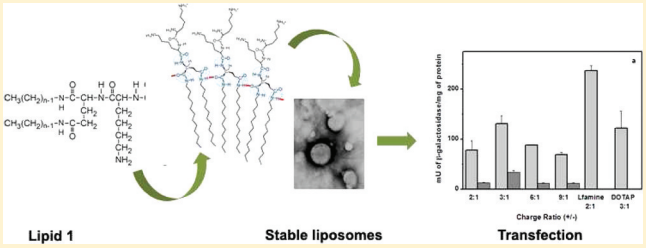

INTRODUCTION

Cationic lipid-based formulations offer attractive solutions for *in vitro* delivery of nucleic acids.[1−4] Liposomes containing cationic lipids electrostatically bind with the polyanionic nucleic acids resulting in a lipoplex that protects nucleic acids from degradation and facilitates endosomal uptake.[5,6] Structurally, cationic lipids are amphiphilic with a hydrophilic cationic headgroup connected with a linker to hydrophobic tails, usually alkyl chains.[7−9] Extensive investigations on chemistry and transfection efficiency of cationic lipids suggest that a wide variety of molecules are suitable when appropriate amphiphilicity is maintained.[5,6] Alkyl chains [8,10] and steroid molecules[11] are a few examples that were found suitable as hydrophobic groups, while a large variety of cationic groups such as primary or tertiary amines together with polyamine and quarternary ammonium,[12,13] guanidino groups,[14] and amino acids[15] were found to enhance transfection efficiency. The enhancement in transfection efficiency in the presence of a neutral lipid or a colipid such as phosphatidylethanolamine or cholesterol was the prime motivation to successfully test a large number of cationic lipids with colipids.

Transfection efficiency by cationic lipids is strongly dependent on the cell type and inclusion of colipids in formulations.[16−18] To obtain insight into the relationship between transfection efficiency and the properties such as size, charge, stability, and interaction with the biological membranes, cationic lipids have been extensively investigated.[15] These studies indicated that compact, fluid, and positively charged lipoplexes overcome serum destabilization, enhanced cellular associations, and eventual escape from the endosomes by fusion.[19] Amino acids or short peptides have been used, especially as headgroup moieties, in the design of cationic lipids.[15] Cationic amino acids lysine and arginine have been extensively used to provide the cationic headgroup[15] to facilitate complexation with the nucleic acids. The pK_a properties of amino acid histidine have been used successfully[20] to cause endosomolysis after uptake of lipoplex. However, use of amino acids as backbone for the cationic lipid has not been investigated. Earlier, we reported

Received: June 3, 2011
Revised: September 19, 2011
Published: October 11, 2011

synthesis and transfection efficiencies of pyridinium-based cationic lipids with glutamide as the backbone.[21] In the design of cationic lipids, linkers are used to connect the headgroup or the hydrophobic portion to the backbone, for example, glycerol.[22−24] This is to provide biodegradability and thereby safety due to decreased toxicities. Ester linkages are preferred over ether linkers[25] primarily for their biodegradability. In some reports, the linkers are designed to enhance the release of the nucleic acid from the lipoplex in response to a change in conditions inside the cell. For example, low pH labile bonds are used to dissociate the headgroup from the lipid in the endosomal compartment and release the plasmid DNA.[13] Reduction of linkers with disulfide bonds in the cytoplasmic milieu destabilizes the complex[26] thereby separating the nucleic acid from the liposomes. Recently, in an otherwise chemically similar lipid, the linker orientation was shown to have dramatic effect on the transfection properties of the lipid.[24] We report in this study two lysinated-glutamide lipids which differ from each other only in their linker chemistry, i.e., either amide or an ester designated as Lipid 1 and Lipid 2, respectively. Lipid 1 with an amide linker melts at a higher temperature and has higher transfection efficiency than the low melting counterpart Lipid 2 with the ester linker. This striking structural difference between the two lipids motivated further investigations to address whether the linker has any role in determining the transfection efficiency.

EXPERIMENTAL PROCEDURES

Materials. In this work, all chemicals and solvents were purchased and used without further purification. The chemical structures of the lipids were identified by melting point, FTIR, ^{1}H NMR, and elemental analysis. Melting points were determined on a micro melting point apparatus. FTIR spectra were performed on a JASCO FT/IR-4000 spectrometer. ^{1}H NMR spectra were recorded by a JEOL JNM-EX400 spectrometer using tetramethylsilane as an internal standard. Elemental analyses were performed with a Yanaco CHN Corder MT-3. ESI-HRMS was performed on a QSTAR XL hybrid MS/MS system (Applied Biosystems/MDS sciex), equipped with an ESI source.

1,6-diphenyl-1,3,5-hexatriene, ethidium bromide, NBD-DHPE, and Rhodamine −DHPE were purchased from Molecular Probes (USA). 1,2-Dioleoyl-*sn*-glycero-3-phosphoethanolamine (DOPE), cholesterol, L-α-phosphatidylglycerol (PG), and 1,2-dioleoyl-*sn*-glycero-3-phosphocholine (DOPC) were purchased from Avanti Polar Lipids (USA). Fluorescein (FAM) Labeling Kits were sourced from Ambion. 3-(4,5-Dimethylthiazol-2-yl)-2,5-diphenyltetrazolium bromide (MTT) and other reagents were purchased from Sigma Co.

Synthesis of Z-Lys(Z)-Lys(Z)-OH. *(A). Z-Lys(Z)-Lys(Z)-OMe.* Z-Lys(Z)-OH (3.42 g, 9.06 mmol), H-Lys(Z)-OMe·HCl (3.0 g, 9.06 mmol), and triethylamine (2.76 g, 27.1 mmol) were dissolved in chloroform. The solution was cooled to 0 °C, and DEPC (1.97 g, 1.09 mmol) was added to the solution and stirred for 30 min at this temperature. After stirring for 1 day at room temperature, the solution was concentrated *in vacuo*, and the residue was dissolved in chloroform. The solution was washed with 0.2 N HCl, 5 wt % $NaHCO_3$, and water. The solution was dried over Na_2SO_4, concentrated, and finally added to diethyl ether, which gave a white solid powder: yield 4.56 g (73%, 6.5 mmol); mp 103−105 °C; FT-IR (KBr) 3316, 2942, 1741, 1690, 1650, and 1542 cm^{-1}; ^{1}H NMR ($CDCl_3$) δ 1.37 (m, 4H, C*HCH$_2$CH_2), 1.49 (m, 4H, CH_2CH_2NH), 1.62 (m, 2H, CHCH_2(CH$_2$)$_3$NH), 1.83 (q, 2H, $CH_3OC(=O)C^*HCH_2$), 3.08−3.18 (m, 4H, C*H-(CH$_2$)$_3$CH_2NHC(=O)), 3.68 (s, 3H, CH_3), 4.18 (s, 1H, $CH_3OC(=O)C^*H$), 4.53 (s, 1H, NHC(=O)C*HNHC(=O)), 5.07 (m, 6H, C*H$_2$Ph), 7.35 (d, 15H, C$_6H_5$). Anal. Found: H, 6.77%; C, 63.4%; N, 7.97%. Calcd. for $C_{37}H_{46}N_4O_9$: H, 6.71%; C, 64.3%; N, 8.11%.

(B). Z-Lys(Z)-Lys(Z)-OH. Z-Lys(Z)-Lys(Z)-OMe (4.6 g, 6.60 mmol) and 1 N NaOH 19 mL (19 mmol) were dissolved in 100 mL methanol, stirred for 1 h at room temperature, and pH was adjusted to 2 by 1 N HCl. After removing methanol from the solution *in vacuo*, the residue was added to ethanol. The obtained white precipitate was removed by filtration, and the solution was concentrated and added to *n*-hexane to give a white precipitate. The precipitate was collected by filtration and dried *in vacuo*: yield 4.30 g (95% 6.35 mmol) mp 145−147 °C; FT-IR (KBr) 3322, 2941, 2863, 1692, 1652, and 1541 cm^{-1}; ^{1}H NMR ($CDCl_3$) δ 1.35 (m, 4H, C*HCH$_2$CH_2), 1.47 (m, 4H, CH_2CH_2NH), 1.63−1.86 (br, 4H, C*HCH_2), 3.10 (d, 4H, C*H(CH$_2$)$_3$CH_2NHC(=O)), 4.26 (s, 1H, HOC(=O)C*H), 4.50 (s, 1H, NHC(=O)C*HNHC(=O)), 5.06 (m, 6H, CH_2Ph), 7.29 (d, 15H, C$_6H_5$). Anal. Found: H, 6.86%; C, 63.44%; N, 8.08%. Calcd. for $C_{36}H_{44}N_4O_9$: H, 6.55%; C, 63.9%; N, 8.28%.

Synthesis of Lipid 1 (2C$_{12}$-Gln-Lys-Lys). *(A). Synthesis of 2C$_{12}$-Gln.* Synthesis of 2C$_{12}$-Gln was described earlier (*Bioconjugate Chem.* **2006**, *17*, 1530).

(B). 2C$_{12}$-Gln-Lys(Z)-Lys(Z)-Z. 2C$_{12}$-Gln (0.93 g, 1.93 mmol), Z-Lys(Z)-Lys(Z)-OH (1.30 g, 1.92 mmol), and triethylamine (0.37 g, 3.84 mmol) were dissolved in dry THF (100 mL). The solution was cooled to 0 °C, and DEPC (0.52 g, 2.88 mmol) was added to the solution and stirred for 1 day at room temperature. After stirring, the solution was concentrated *in vacuo*, and the lipid was recrystallized from ethanol, which gave a white solid powder: yield 1.07 g (50%, 0.94 mmol); mp 184−187 °C; FT-IR (KBr) 3295, 2925, 2853, 1693, 1637, and 1543 cm^{-1}; ^{1}H NMR ($CDCl_3$) δ 0.86−0.89 (t, 6H, CH_3), 1.25 (m, 36H, CH$_3$(CH_2)$_9$), 1.33 (s, 4H, CH_2CH$_2$NHC(=O)), 1.48 (br, 6H, C*H(CH_2)NHC(=O)), 1.58−2.40 (s, 8H, C*HCH$_2$CH_2CH$_2$, C*HCH$_2$CH$_2$CH_2), 2.44 (m, 2H, C*HCH$_2$CH_2C(=O)), 3.16−3.23 (br, 8H, CH_2NHC(=O), CH_2NHC(=O)O), 4.11 (s, 1H, C*HNHC(=O)), 4.35 (s, 1H, C*HNHC(=O)), 4.51 (s, 1H, C*HNHC(=O)), 4.92−5.15 (br, 6H, CH_2Ph) 7.28−7.34 (m, 15H, C$_6H_5$). Anal. Found: H, 8.94%; C, 68.3%; N, 8.56%; Calcd. for $C_{65}H_{101}N_7O_{10}$: H, 8.93%; C, 68.5%; N, 8.60%.

(C). 2C$_{12}$-Gln-Lys-Lys. 2C$_{12}$-Gln-Lys(Z)-Lys(Z)-Z (0.93 g, 0.82 mmol) was dissolved in 100 mL ethanol with heating, and Pd/carbon (0.5 g) was added to the solution. H_2 gas was bubbled slowly into the solution for 14 h at 70 °C. Pd/carbon was removed by filtration, and the solution was dried *in vacuo* to give a solid powder: yield 0.34 g (52%, 0.43 mmol, as a trihydrate); mp 104−107 °C; FT-IR (KBr) 3289, 2920, 2851, 1639, and 1557 cm^{-1}; ^{1}H NMR ($CDCl_3$) δ 0.87−0.90 (t, 6H, CH_3), 1.28 (m, 36H, CH$_3$(CH_2)$_9$), 1.52−2.17 (br, 20H, CH_2CHNHC(=O), CH_2C*H, CH_2CH$_2$C*H, CH_2(CH$_2$)$_2$C*H), 3.12−3.35 (br, 8H, CH_2-NHC(=O), CH_2NHC(C=O)O), 4.31−4.56 (br, 3H, C*HNHC(=O)). Anal. Found: H, 10.9%; C, 64.9%; N, 11.4%. Calcd. for $C_{41}H_{89}N_7O_7$: H, 11.3%; C, 62.2%; N, 12.4%. ESI-HRMS: m/z = +738.6569 (calcd value for $C_{41}H_{84}N_7O_4$ = 738.6584).

Synthesis of Lipid 2 (2C$_{12}$Glu-Lys-Lys). *(A). Didodecyl-L-Glutamate Toluene-p-Sulfonate (2C$_{12}$L-Glu TosOH).* L-Glutamic acid (6.0 g, 40.0 mmol), *p*-toluenesulfonic acid

(6.82 g, 48.0 mmol), and 1-dodecanol (17.8 g, 96.0 mmol) were dissolved in toluene (250 mL), and refluxed for 5 h by use of Dean−Stark apparatus. The solution was concentrated in vacuo, and the residue was dissolved in 200 mL of diethyl ether, and refrigerated to 4 °C for 1 day, which gave a white solid powder: yield 13.1 g (49%), mp 65−66 °C. Anal. Found: H, 9.93; C, 65.4; N, 2.40; Calcd. for $C_{36}H_{65}NO_7S$: H, 9.99; C, 65.9; N, 2.14. FT-IR (KBr) 2921 cm^{-1} (ν_{C-H}), 2850 cm^{-1} (ν_{C-H}), 1743 cm^{-1} (ν_{ester}), 1533 cm^{-1} (δ_{NH}), 1182 cm^{-1} (ν_{C-O}). ^1H NMR ($CDCl_3$, internal reference: tetramethylsilane) δ 0.86−0.90 (m, 6H, CH_3) δ 1.26 (m, 36H, CH_3-$(CH_2)_9$), δ 1.55 (m, 4H, $CH_2CH_2OC(=O)$), δ 2.15−2.25 (m, 2H, $C^*HCH_2CH_2C(=O)$), δ 2.34 (s, 1H,CH_3Ph), δ 2.43−2.58 (m, 2H, $C^*HCH_2CH_2C(=O)$), δ 3.95−4.11 (m, 4H, $CH_2CH_2OC(=O)$), δ 7.12−7.14 (d, 2H, C_6H_5), δ 7.72−7.74 (d, 2H, C_6H_5).

(B). $2C_{12}$Glu-Lys(Z)-Lys(Z)-Z. $2C_{12}$Glu-Lys(Z)-Lys(Z)-Z was synthesized by similar method with $2C_{12}$Gln-Lys(Z)-Lys(Z)-Z: yield 1.20 g (51%); mp 130−131.5 °C; FT-IR (KBr) 3307 cm^{-1} 2924 cm^{-1} (ν_{C-H}), 2853 cm^{-1} (ν_{C-H}), 1732 cm^{-1} ($\nu_{C=O(ester)}$), 1688 cm^{-1} ($\nu_{C=O(urethan)}$), 1640 cm^{-1} ($\nu_{C=O(amide)}$), 1543 cm^{-1} (δ_{N-H}), ^1H NMR ($CDCl_3$) δ 0.86−0.90 (m, 6H, CH_3), δ 1.26 (m, 40H, CH_3-$(CH_2)_9$, $C^*HCH_2CH_2CH_2$), δ 1.49 (m, 4H, $CH_2CH_2NHC(=O)$), δ 1.56 (m, 4H, $CH_2CH_2OC(=O)$), δ 1.68−1.88 (br, 4H, $CH_2C^*HNHC(=O)$), δ 1.94−2.01(m, 1H, $C^*HCH_2CH_2C(=O)$), δ 2.11−2.16 (m, 1H, $C^*HCH_2CH_2C(=O)$), δ 2.36 (m, 2H, $C^*HCH_2CH_2C(=O)$), δ 3.16 (m, 4H, $CH_2CH_2NHC(=O)$), δ 4.03 (m, 4H, $CH_2CH_2OC(=O)$), δ 4.15 (m, 1H, $CH_2OC(=O)C^*HNH$ $C(=O)$), δ4.38 (q, 1H, $NHC(=O)C^*HNH$ $C(=O)$), δ 4.53 (q, 1H, $NHC(=O)C^*HNH$ $C(=O)OCH_2Ph$), δ 5.07 (m, 6H, $PhCH_2OC(=O)$), δ 7.31 (d, 15H, C_6H_5). Anal. Found: H, 8.69; C, 67.8; N, 6.20; Calcd. For $C_{65}H_{99}N_5O_{12}$: H, 8.73; C, 68.3; N, 6.13.

(C). $2C_{12}$-Glu-LysLys. $2C_{12}$Glu-LysLys was synthesized by similar method with $2C_{12}$Gln-LysLys: yield 0.40 g (49%, 0.47 mmol, as a hexahydrate); FT-IR (KBr) 3307 cm^{-1} and 2925 cm^{-1} (ν_{C-H}), 2854 cm^{-1} (ν_{C-H}), 1737 cm^{-1} ($\nu_{C=O(ester)}$), 1654 cm^{-1} ($\nu_{C=O(amide)}$), 1557 cm^{-1} (δ_{N-H}), ^1H NMR ($CDCl_3$) δ 0.86−0.90 (m, 6H, CH_3), δ 1.27 (m, 36H, $CH_3(CH_2)_9$), δ 1.50−2.27 (br, 18H, CH_2), δ 2.51 (m, 2H, $C^*HCH_2CH_2C(=O)$), δ 3.15 (m, 4H, CH_2-NH_2), δ 4.14−4.20 (m, 4H, $CH_2CH_2OC(=O)$), δ 4.30−4.57 (br, 3H, $C^*HNHC(=O)$). Anal. Found: H, 9.4; C, 58.1; N, 8.00. Calcd. for $C_{41}H_{93}N_5O_{12}$: H, 11.1; C, 58.1; N, 8.26. ESI-HRMS: m/z = +740.6245 (calcd value for $C_{41}H_{82}N_5O_6$ = 740.6265).

Preparation of Liposomes. Cationic amphiphiles Lipid **1**, **2**, and the colipid cholesterol were dissolved in chloroform and mixed in glass vials at 1:1 mol ratio. Chloroform was then removed with a thin flow of nitrogen and the dried lipid film was kept under vacuum for 4−5 h. Subsequently, deionized water was added to the dried lipid film for overnight rehydration. The vial was vortexed thoroughly at RT to produce multilamellar vesicles (MLVs). MLVs were sonicated until clarity to obtain small unilamellar vesicles (SUV).

DNA-Binding Assay. *Agarose Gel Electrophoresis.* Plasmid $pGFPN_3$ was complexed with cationic lipids at charge ratios varying from 0.3:1 to 3:1 (lipid/DNA) to measure the DNA binding ability. In a typical binding assay, 0.6 nmol of DNA, corresponding to 200 ng of plasmid DNA, was complexed with the lipids, at indicated charge ratios, in 10 mM phosphate buffer (pH 7.5), deionized water or 0.5× PBS in a volume of 20 μL and incubated at room temperature for 30 min. After addition of the tracking dye bromophenol blue, samples were directly loaded on a 1% agarose gel with TAE buffer and electrophoresed at 80 V for approximately 2 h. The gel was stained with ethidium bromide (EtBr), post electrophoresis, and visualized under a transilluminator. DNA binding was also carried out by EtBr fluorescence titrations as described.[27]

Ethidium Bromide (EtBr) Fluorescence Quenching. The binding of DNA with Lipid **1** and **2** was studied using EtBr as the fluorescent probe. The lipids were reconstituted with colipids DOPE or cholesterol in deionized water using standard protocols. Bound EtBr was expelled from the DNA−EtBr complexes by the lipid. This displacement of EtBr is reflected as a drop in the fluorescence signal, since unbound EtBr does not fluoresce. All fluorescence measurements were carried out using a Hitachi F-4500 fluorescence spectrophotometer. The excitation wavelength, λ_{ex}, was 516 nm and the emission wavelength was kept at 598 nm (slit width 5 × 5 nm^2). Briefly, 2.3 μg of pCMV-β-gal plasmid DNA was added to 500 μL of 20 mM Tris−HCl buffer (pH 7.4) in a fluorescence cuvette. EtBr 0.23 μg, from a diluted stock solution, was added to DNA and the baseline fluorescence was determined. The fluorescence intensity obtained upon each addition of lipid was normalized relative to the fluorescence signal of DNA−EtBr complex, in the absence of the lipid, which was taken as 100%. The binding of DNA by the lipid was recorded after each addition at time intervals of 5 min.

Transfection. CHO, HepG2, cells were plated at a density of 10 000 cells per well in a 96-well plate on the previous day. Plasmid DNA pCMVβ-gal was purified by using the Qiagen Kit (endotoxin free) using the manufacturer's protocol and also by CsCl−EtBr density gradient ultracentrifugation using standard protocols. Plasmid (0.9 μg corresponding to 2.72 nmol) was complexed with varying amounts of Lipid **1** and **2**, formulated with cholesterol at 1:1 mol ratio, to obtain charge ratios varying from 1:1 to 9:1, DNA/Lipid, in DMEM without serum and incubated at RT for 30 min. Complexes were added to cells after appropriate dilution with DMEM to achieve 0.3 μg per well, and incubated for 3 h. The medium was then replaced with complete medium containing 10% serum.

Serum stability experiments were performed as described[21] in CHO and HepG2 cells. Briefly, transient transfections, *in vitro*, were done in the presence of fetal calf serum. Lipid/DNA complexes were prepared in the absence of serum and incubated for a period of 30 min at room temperature. Serum was then added to the complex to obtain the 10% final concentration and then added to the cells, seeded on a 96-well plate and the charge ratios varied from 2:1 to 12:1 Lipid/DNA. Data is represented as β-gal activity/well (20 000 cells). Reporter gene assay was carried out 48 h post transfection and efficiency depicted as relative β-gal activity. In these assays, cells were washed with PBS and lysed in 50 μL of lysis buffer (0.25 M Tris.HCl, pH 8.0, and 0.5% NP40). β-Gal activity was estimated by adding 50 μL of 2× substrate (1.33 mg/mL ONPG, 0.2 M sodium phosphate, pH 7.15, and 2 mM magnesium chloride) to an equal volume of the lysate in a fresh 96-well plate and incubated at 37 °C. Absorption at 405 nm was converted to β-gal units by using a standard curve generated with pure commercial enzyme.

Differential Scanning Calorimetry. Thermal transitions in Lipids **1** and **2** were performed using VP-DSC MicroCal calorimeter (VP-ITC model). The calorimetry was performed using Lipids **1** and **2** (8.8 mg/mL) vesicles prepared in deionized water as described above except the sonication step. All samples (250 μL) were degassed before acquiring the scans

which were performed between 10 °C and 95 ° C at a scan rate of 60 deg/h. Water or buffer baselines were obtained and subtracted from lipid scans.

Fluorescence Anisotropy Measurements. These measurements were carried out using Fluorolog 3−22 Fluorescence Spectrophotometer (Jobin Yvon,USA). Lipids **1** and **2** were prepared from chloroform stocks by the appropriate addition of the fluorescent probe DPH (1,6-diphenyl-1,3,5-hexatriene) at 300:1 mol ratio of Lipid/DPH, to obtain 2 mM stock of the lipid. This mixture was then dried under nitrogen gas. The residual chloroform was then removed in a vacuum for 4 h. Lipid films were then hydrated in 1 mL of buffer (Tris. HCl, pH 7.4, 100 mM) overnight, vortexed, and sonicated prior to the scans between 15 and 90 °C with 2.5 °C increments. Fluorescence anisotropy was measured by recording the DPH fluorescence values (excitation at 354 nm and emission at 427 nm) in parallel and perpendicular polarizer positions. Anisotropy values were calculated by instrument software.

Membrane Fusion. Membrane fusion between cationic lipid vesicles and anionic vesicles was monitored by Förster resonance energy transfer (FRET) between NBD-PE and Rhodamine DHPE. The liposomes containing the fluorophores were prepared with the following composition: DOPC:DOPE:egg PG:NBD-PE:Rh-PE at a mole ratio of 75:20:5:0.8:0.8. Cationic liposomes were prepared with Lipid **1** and **2** along with cholesterol in a mole ratio of 50:50. The fusion was initiated by mixing 50 nmol of cationic lipid vesicles with 10 nmol of fluorescent lipids in phosphate buffered saline (10 mM sodium phosphate buffer, pH 7.4, with 150 mM of sodium chloride) at 25 °C in stirring conditions. The increase in fluorescence was monitored in a Hitachi F4300 spectrofluorimeter by exciting the sample at 460 nm and collecting the emission at 530 nm. The total fluorescence was measured by adding Triton X-100 at a final concentration of 0.15%. The small but measurable quenching due to Triton X-100 was corrected. Anionic vesicles were also prepared using phosphatidic acid instead of PG at the same mole ratio, and we obtained similar results.

Surface Area−Pressure Isotherms. The measurements were made on a Langmuir trough manufactured by Nima (model 622D) using high-purity water as subphase. Lipids **1** and **2** were prepared as stocks in chloroform and spread at the air−water interface in less than 5 μL. The pressure−area isotherms were obtained at compression rates of 50 cm^2 per minute. Since the surface area available with the trough does not allow us to monitor the collapse point of the monolayer, only the rate of change of the surface pressure for change in molecular area was used in the study.

Transmission Electron Microscopy. SUVs of Lipids **1** and **2** (2 mM) were prepared as described earlier. The vesicle solution was cast on the poly(vinyl acetate)-coated copper grid and stained with 1.0 wt % uranyl acetate aqueous solution. The TEM images were recorded by JEM-2000EX/FX (JEOL, Co. Ltd.) with 80 kV accelerating voltage.

Live Uptake of DNA by Confocal Microscopy. Chambered cover glass was plated with 20 000 cells (CHO) and incubated with lipoplexes (with 6:1 lipid/DNA charge ratio) prepared with Lipids **1** and **2** in 300 μL of DMEM containing Oregon Green-labeled plasmid pCMVβ-gal plasmid DNA prepared as described. After the incubation period of 3 h, DMEM was removed, and the cells were washed with PBS twice before obtaining images (Leica TCS S52). The cells containing labeled DNA (ChromaTide Oregon Green 488−5′dUTP): RhDHPE-labeled lipid complexes were visualized using the 488 nm excitation of argon laser, 405 nm excitation of diode while Rhodamine was detected using HeNe excitation wavelength of 543 nm. The emission collection wavelengths were 500−540 nm for Oregon Green, 415−485 nm for Hoechst 33258, and 560−615 nm for Rhodamine. In each panel, 5 slices of 0.5 μm were combined. Last panel indicates overlaid images depicting nuclear staining with Hoechst 33258.

Toxicity Assay. Cytotoxicity of the Lipids **1** and **2** were assessed in CHO cells using 3-(4,5-dimethylthiazol-2-yl)-2,5-diphenyltetrazolium bromide (MTT). Complexes prepared with lipid, were evaluated for their toxicity to cells by performing the MTT assay as described[27] in 96-well plates at charge ratios used in the transfection experiments. Cells were incubated with transfection complexes for 3 h at 37 °C in serum-free DMEM. Soon after transfection, cells were washed with PBS and replaced with 100 μL DMEM+25 μL MTT (2 mg/mL in PBS) for 3 h. The medium was removed and replaced with 100 μL DMSO/methanol 1:1 (v/v) and mixed to dissolve the formazan crystals. Absorbance was then measured at 540 nm with untreated cells serving as controls. Results were expressed as percent viability. [A540 (treated cells) − background/A540 (untreated cells) − background] × 100.

Small Angle X-ray Diffraction of the Lipid Vesicles. Vesicles of Lipids **1** and **2** with cholesterol were prepared as described above. The lipid concentration for SAXS studies was 5 mM and vesicles were used without sonication. Diffraction data were collected on a S3-MICROpix attached to a Dectris 100K Platus detector (Hecus Xray Systems, Graz, Austria) located 300 mm from the sample. Detector was precalibrated with silver behenate. Samples were filled in 1 mm thin-walled quartz-glass capillaries in tight thermal contact with a programmable Peltier unit. Samples were equilibrated for 10 min at each temperature before measurement. The data were fitted using *Fit2d* software.[28]

RESULTS

Synthesis of the Lipids. To investigate the role of the amide and ester linker in a cationic lipid on transfection properties, $2C_{12}$Glu and $2C_{12}$-Gln were synthesized and later coupled to Z-Lys (Z)-Lys(Z)-OH. The schemes for the synthesis of Lipid **1** (amide lipid) and Lipid **2** (ester lipid) is given in Scheme 1A,B. The purity was assessed by HPLC and chemical nature of the compounds was confirmed by FTIR, ^{1}H-NMR, and elemental analysis.

DNA Binding Properties of Lipid 1 and 2. *Agarose Gel Retardation Assay.* We initially investigated the DNA-binding ability of Lipid **1** and **2** by a gel-based assay. Both lipids formulated with cholesterol bind to plasmid DNA, pEGFPN$_3$ (Figure 1A). Formation of a complex and its retardation was observed with Lipids **1** and **2** with cholesterol as the colipid at 0.3:1 charge ratio. At charge ratios greater than 2:1, the complexes were either retained in the well or not amenable to EtBr binding after electrophoresis. The binding of lipids with the plasmid was found to be ratio-dependent. The binding of Lipid **1** was more avid compared to Lipid **2** when formulated with DOPE (data not shown). Therefore, only formulations with cholesterol were taken up for further biophysical investigations and cell biological activity *in vitro*.

Fluorescence Quenching. Binding strengths of cationic lipids with DNA are important to correlate the transfection properties of lipids to its chemical structure. Exclusion of EtBr

Scheme 1. A. Synthesis Scheme and Structure of Glutamide Lipid 1 (n = 12) with the Amide Linker. B. Synthesis Scheme and Structure of Lipid 2 (n = 12) with Ester Linker

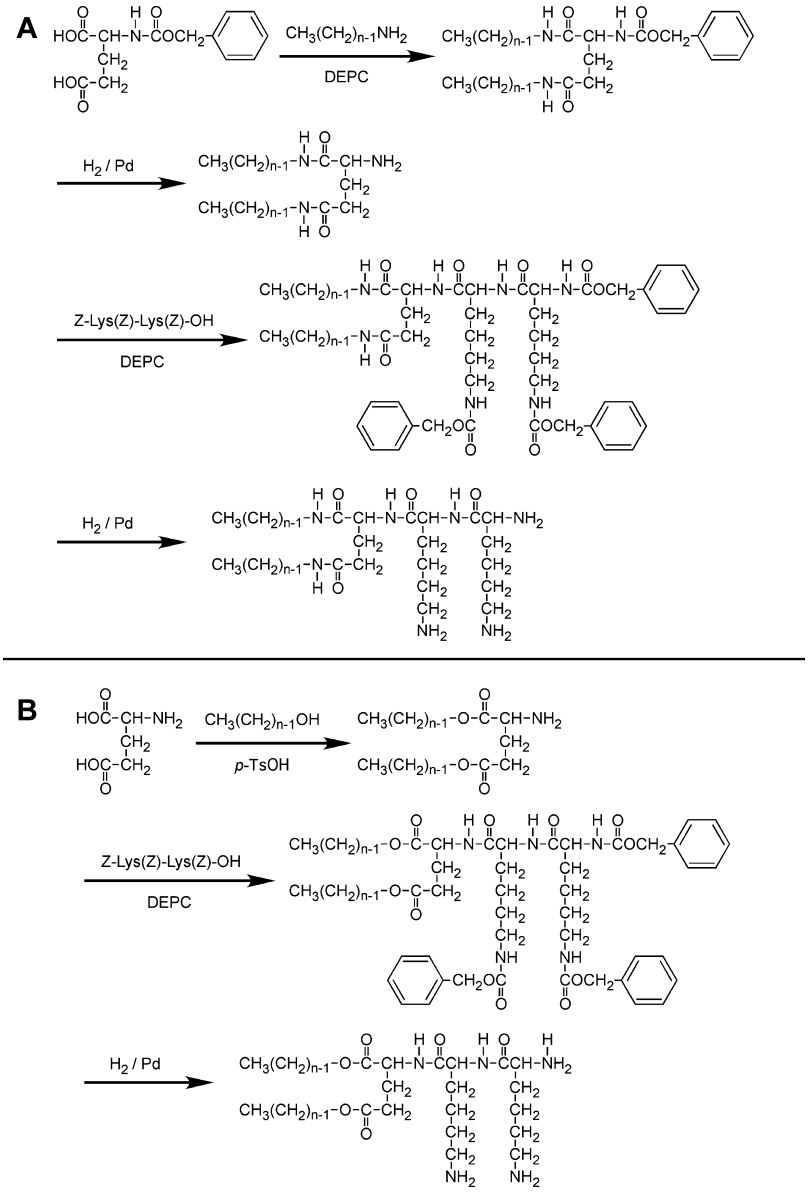

from DNA upon the addition of cationic lipid, and consequent enhancement of fluorescence, provides a sensitive and quantitative measurement for DNA binding. Figure 1B shows the DNA binding pattern of Lipid **1** in comparison to Lipid **2**, which was similar at lower charge ratios. However, at charge ratios above 1:1, Lipid **1** shows a slightly stronger binding with ~25% drop in the fluorescence intensity when compared to ~17% decrease with Lipid **2**.

Uptake of Lipoplexes in CHO Cells. We examined the cellular uptake of lipoplexes prepared with Lipid **1** and Lipid **2** formulated with cholesterol in CHO cells. An Oregon-Green labeled plasmid probe (green) was mixed with an equal proportion of unlabeled DNA to prepare lipoplexes labeled with 0.5 mol % of fluorescent lipid (RhDHPE), at the charge ratios indicated and added to CHO cells followed by incubation at 37 °C for 3 h. After thorough washes with DMEM, live cells were viewed by confocal microscopy. The upper panel, i.e., Lipid **1** (Figure 2), exhibited particulate bright red fluorescence originating from the Rhodamine-labeled lipid that colocalized with the labeled-plasmid DNA. Uptake of Lipid **2** was comparatively less (see merged panel of this figure). Quantitative analysis of the confocal image was done by measuring mean fluorescence intensity (MFI) per cell using *LAS AF* software. When compared with Lipid **2**, we observed a 3-fold increase in the MFI measured either by OG-labeled DNA or Rhodamine-labeled liposomes in the uptake of lipoplexes prepared with Lipid **1**/Chol.

Biophysical Characterization of the Lipids. *Determination of the Melting Temperature of the Lipids.* Hydrated lipid samples with and without the colipid, cholesterol, were subjected to thermal transitions in a differential scanning calorimeter (DSC). The heat capacity changes in the lipid phase as a function of temperature were plotted in Figure 3. The transition midpoints were found to be 65.4 and 23.5 °C for Lipid **1** and **2**, respectively. Similar transition midpoints was also found for these lipids in the presence of cholesterol. The transition midpoint for lipids is known to be determined by the chain length of the alkyl group. Since both lipids have identical chain length (C12) and identical head groups, the higher

dx.doi.org/10.1021/bc2002874 | *Bioconjugate Chem.* 2011, 22, 2244–2254

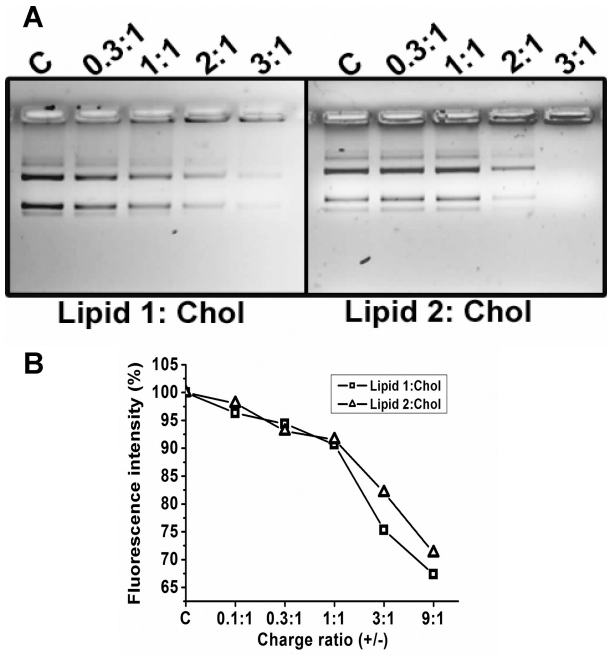

Figure 1. Binding of DNA with Lipids **1** and **2** in the presence of the colipid cholesterol: (A) 1% Agarose gel electrophoresis of plasmid pCMVβ-gal complexed with Lipids **1** and **2** at charge ratios varying from 0.3:1 to 3:1 Lipid/DNA, indicated above each well. Samples were electrophoresed using TAE buffer (pH 8.0) and visualized post-electrophoresis by staining with EtBr. Control in each panel denoted as "C" pertains to naked plasmid DNA. (B) Fluorescence quenching by EtBr exclusion assay of Lipids **1** and **2** formulated with colipid cholesterol. Fluorescence titration curves depict quenching of fluorescence due to release of EtBr from pCMVβ-gal plasmid DNA upon lipid binding in a buffer containing 20 mM Tris·HCl (pH 7.4).

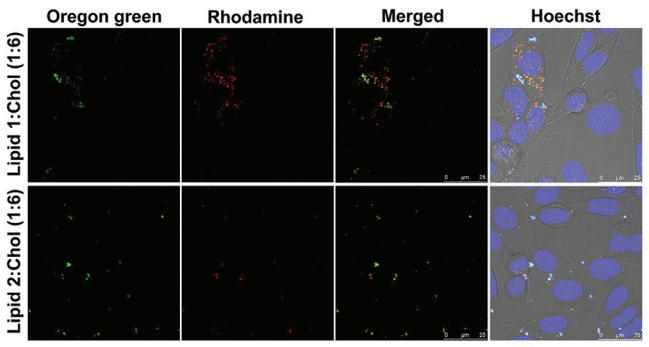

Figure 2. Uptake of lipoplexes and analysis by confocal microscopy: Transfection complexes with the corresponding lipid were added to cells in the absence of serum and incubated for 3 h. Lipid **1**/Chol at 6:1 DNA/Lipid (top) and Lipid **2**/Chol at 6:1 DNA/Lipid (bottom). DNA was labeled with Oregon-Green while liposomes were labeled with Rhodamine DHPE at 0.5 mol %. The merged panel indicate colocalization of the fluorophores. Cell nuclei were stained with Hoechst (blue). Panels on the extreme right depict images merged with the transmission channel. Five optical sections in the middle region, each of 0.5 μm thickness, were combined to generate the images.

melting temperature of Lipid **1** may have been due to additional interactions in Lipid **1**. To confirm the phase transitions, we used identical preparations of Lipid **1** and **2** with a fluorescent probe diphenyl hexatriene (DPH) at 300:1 ratio (lipid/DPH, mol/mol). Anisotropy of DPH is sensitive to the microviscosity of its location. DPH resides at the center of the bilayer and its

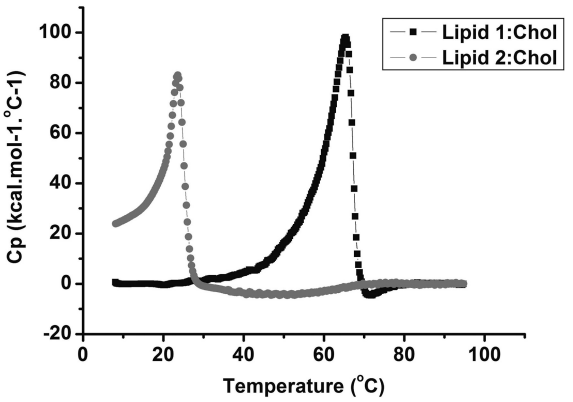

Figure 3. Differential scanning calorimetric scans of lipid vesicles: Thermograms of Lipid **1** and Lipid **2** formulated with equimolar amounts of cholesterol. Vesicles were prepared as described in methods.

anisotropy has been extensively used to estimate the phase transition temperatures of lipid assemblies. Lipid **1** exhibited a sharp phase transition around 67 °C, whereas Lipid **2** had a shallow transition at lower temperatures (Supporting Information Figure 1S). Thus, a higher melting temperature of Lipid **1** was confirmed by two independent methods.

Transmission Electron Microscopy (TEM). Having determined the melting temperature of liposomes of Lipids **1** and **2**, we sought to examine the structural features of these liposomes by transmission electron microscopy (TEM). The images obtained with Lipid **1** vesicles prepared with cholesterol or DOPE as the colipid at charge ratio 3:1 revealed the formation of very well-defined spherical structures with a clear inside–outside demarcation. The average size of the vesicles was between 100 and 200 nm in diameter. In contrast, liposomes prepared with Lipid **2** with either of the colipids resulted in supramolecular assemblies that were fragmented and poorly defined (Figure 4). The liposomal preparation with Lipid **2** resulted in structures with long continuous layers that were not discrete. Liposomes of Lipid **1** had unaltered morphology when the particles were prepared either in water or in the presence of PBS (ionic strength = 0.154) (data not shown).

To confirm our observations further, we subjected both the liposomal samples to small angle X-ray scattering (SAXS). SAXS provides information on characteristics of long-range-ordered structures and has been extensively used in identifying the phase properties of the lipids in membranes. The SAXS pattern of Lipids **1** and **2** as shown in Figure 5 indicated defined scatter peaks for Lipid **1** with ordered assembly, and the simulation fitted the scatter to ordered lamellar structures. The scatter profile of liposomes prepared with Lipid **2** resulted in a broad scatter peak indicative of an amorphous material. The peak distances in the scattergram were used to calculate the d_1 (thickness of the membrane). We obtained 3.58 nm for the thickness of the Lipid **1**. We obtained similar distance for Lipid **2** though the peak peak intensities were significantly smaller in case of this lipid. The thickness saturated phosphatidylcholine of 12-carbon chains gives a thickness of 3.0 nm, which is comparable with Lipid **1**. The results of SAXS confirm the absence of organized structure in the liposomes of Lipid **2**.

Compressibility of Lipid Monolayers. With a view to investigate the higher melting temperature of Lipid **1**, we spread both lipids on water subphase and monitored the changes in surface pressure as a function of area occupied by the molecule

dx.doi.org/10.1021/bc2002874 | *Bioconjugate Chem.* 2011, 22, 2244–2254

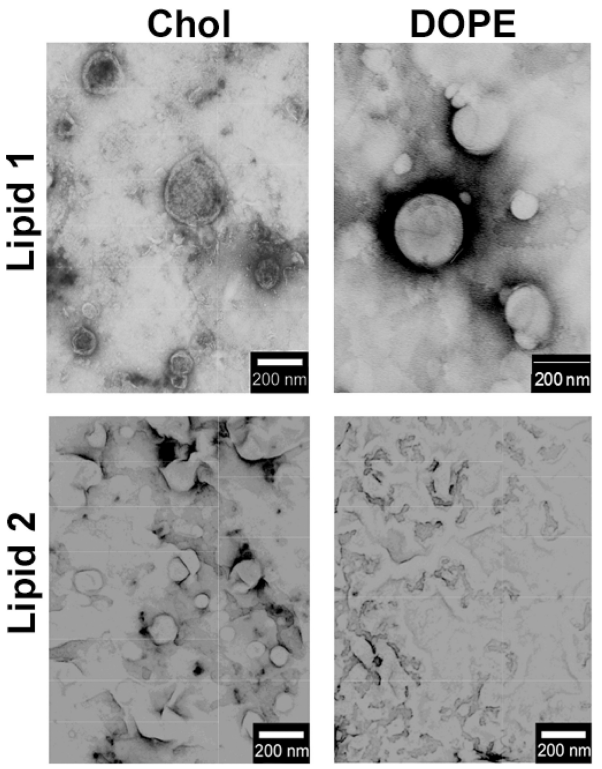

Figure 4. Transmission electron micrographs of Lipids **1** and **2**: Lipids formulated with DOPE or cholesterol were complexed with plasmid pCMV*β*-gal DNA in 1× PBS buffer at Lipid/DNA 6:1 charge ratio. Lipoplexes were stained with uranyl acetate as described.

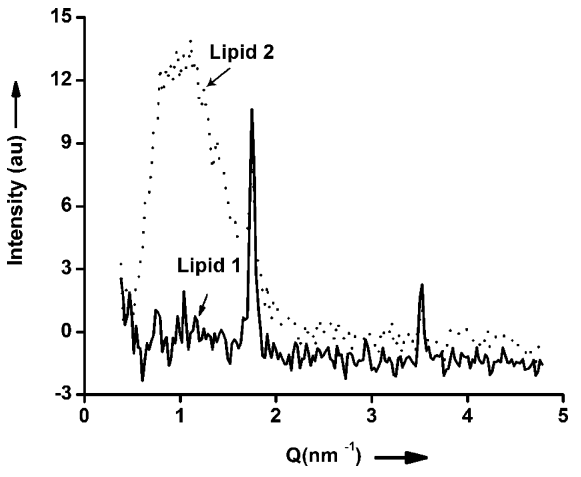

Figure 5. Small-angle X-ray diffraction of lipid vesicles: Vesicles of Lipids **1** and **2** formulated with cholesterol were prepared. The lipid concentration was kept at 5 mM and used without sonication. Diffraction data were collected and fitted using *Fit2d* software.

(Figure 6). Surface pressure vs area isotherms of monolayers of lipids provides information on the surface areas and intermolecular interactions. The slow compressibility of Lipid **1** compared to that of Lipid **2** suggested that the Lipid **1** monolayer experiences additional resistance to compression compared to Lipid **2**. This resistance may possibly be attributed to additional interactions between molecules.

Fusion Properties with Anionic Liposomes. Fusion of the membrane components of the lipoplex membrane with the

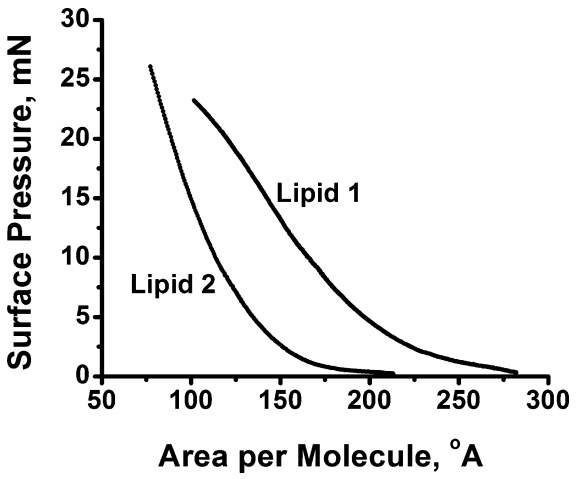

Figure 6. Surface pressure isotherms of Lipids **1** and **2** were generated in the presence of high-purity water as the subphase. Isotherms are representative of four independent measurements with very good reproducibility between the isotherms.

cellular membrane is critical for release of DNA. We monitored the fusion between cationic liposomes of both lipids along with the anionic vesicles prepared with a composition similar to the plasma membrane. The fusion kinetics was monitored using FRET between the donor, NBD-PE, and the acceptor, Rh-PE. Lipid **2** as seen in Figure 7 showed rapid increase in fluorescence

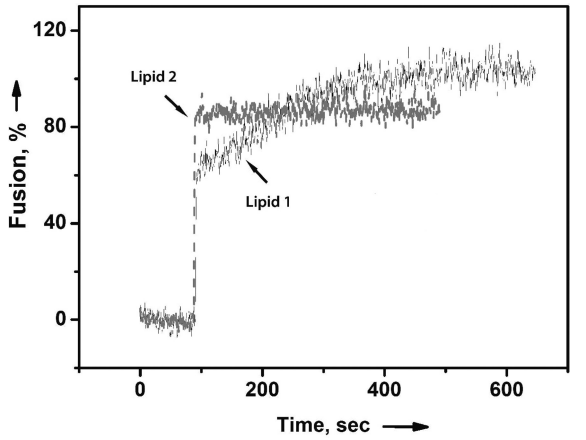

Figure 7. Membrane fusion kinetics: Membrane fusion between anionic vesicles with Lipid **1** or Lipid **2** was monitored by fluorescence resonance energy transfer between NBD-PE and Rhodamine PE, as described.

signal and reached a value representative of complete mixing, i.e., in the presence of Triton X-100, within 1 min. Many variations employed in the experimental design such as the ratio of labeled and unlabeled vesicle and composition of the labeled vesicles did not change the kinetics. Since Lipid **2** has poorly defined vesicles as seen in TEM, it is possible that these vesicles were unstable, hence show very rapid increase in fluorescence that was not typical of a fusion process. On the other hand, Lipid **1** shows comparatively slower kinetics of fusion with labeled vesicles. The fusion kinetics was similar when the labeled vesicles were prepared with phosphatidic acid instead of phosphatidylserine (data not reported).

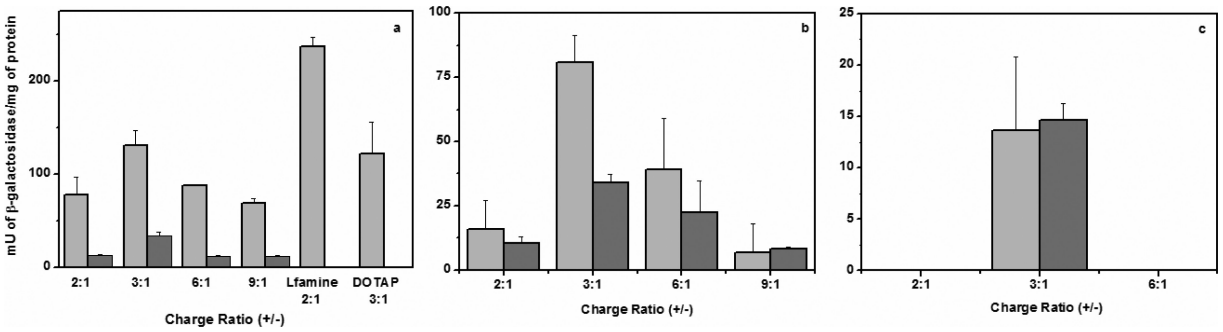

Figure 8. Transient transfection *in vitro*: (a) Transfection of CHO cells with Lipid **1** formulated with equimolar amounts of the colipid, cholesterol, at charge ratios varying from 2:1 to 9:1 Lipid/DNA in the absence (light gray) and presence of serum (dark gray) and normalized to milligrams protein. Graph depicts reporter gene activity at various charge ratios. Standards such as Lipofectamine (Lfamine) and DOTAP at 2:1 and 3:1 charge ratio, respectively, were included for comparison. Lipid **2** did not show any detectable reporter gene activity on CHO cells and was not plotted. (b) Transfection in HepG2 cells with Lipid **1**/Chol at the indicated charge ratios in the absence (light gray) and presence of serum (dark gray). (c) Transfection in HepG2 cells with Lipid **2**/Chol at the indicated charge ratio in the absence (light gray) and presence of serum (dark gray).

Biological Activity and Stability in Serum. *Transient Transfection in CHO and HepG2 Cells.* The lipids initially characterized for their DNA-binding properties were then tested for transfection efficiency in four cell lines, namely, CHO, HepG2, MCF-7, and HeLa. Both the lipids were formulated with DOPE or cholesterol as colipid and tested for transfection efficiency. Formulations with DOPE as colipid were consistently lower than formulations with cholesterol as colipid (data not shown), when tested in CHO cells. Hence, in all further studies only cholesterol-containing liposomes were used. Transient transfections of the two lipids at varying charge ratios from 2:1 to 9:1 Lipid/DNA, using pCMVβ-gal as the reporter gene, were performed as described in CHO cells (Figure 8a) and HepG2 cells (Figure 8b and c). When compared with the cationic lipid standards, i.e., DOTAP/DOPE and polycationic lipid, Lipofectamine, we observed slightly better transfection than DOTAP, and the efficiency was 50% of the transfection observed with Lipofectamine. We also tested the 14- and 16-carbon analogues of Lipid **1**, which is 12-carbon, and found that Lipid **1** has shown higher transfection than the 14- and 16-carbon analogues, >3-fold, Supporting Information Figure 2S. As in the case of HepG2, Lipid **1** (Figure 8b) exhibited much higher activity than Lipid **2** (Figure 8c). Lipid **2** was inefficient in all cell lines tested. The biological activity of Lipid **1** with the amide linkage was consistently higher than that of Lipid **2** that is ester-based in both HeLa cells Supporting Information Figure 3S and MCF-7 (data not reported). In all cell lines, maximal activity was observed at 3:1 Lipid/DNA with Lipid **1** formulated with cholesterol.

Although lipids bind DNA by charge−charge interaction, these may not protect DNA sufficiently from degradation by nucleases. Stability in serum is an important property when developing protocols for *in vivo* gene transfer. To assess the serum stability of Lipid **1**, serum was included in the medium, to a final concentration of 10%, at the time of incubation of cells with the complexes. As evident from Figure 8a−c, compared to the controls, i.e., in the absence of serum, Lipid **1** retained approximately 25% of its transfection efficiency in the presence of serum at 10% final concentration in CHO and 40−57% in the case of HepG2 cells at all charge ratios. Transfection decreased further in the presence of serum concentrations greater than 10%. Lipid **2** has observable but low transfection in HepG2 cells at 3:1 charge ratio and good stability in the presence of serum (Figure 8c). Overall, the transfection efficiency in the presence and absence of serum has a similar bell-shaped curve as a function of charge ratio.

Toxicity. Toxicity is an important issue to be dealt with while generating formulations useful for gene delivery protocols. We performed MTT-based cell viability assays at various charge ratios, i.e., 1:1 to 9:1 in CHO cells. Percent cell viabilities upon treatment with Lipid **1** at charge ratios 3:1 is ∼70% (Figure 9).

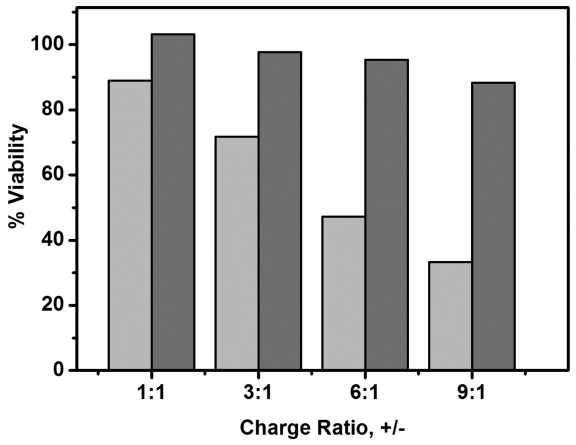

Figure 9. Determination of cell viability in CHO cells. Lipid **1** and **2**:DNA:Lipid complexes of Lipids **1** and **2** formulated with cholesterol was evaluated for cytotoxicity at the indicated charge ratios varying from 1:1 to 9:1 N/P. Following 3 h incubation, the MTT assay was performed. Percent cell viability represents experiments performed in triplicate as described in Materials and Methods. The absorption values obtained using reduced formazan, in the absence of lipids, were taken to be 100.

In contrast, Lipid **2** is inefficient at this charge ratio, although nontoxic. The utility of Lipid **1**/cholesterol offsets the observed toxicity making it effective *in vitro*.

DISCUSSION

Two glutamic acid-based lipids that have identical head groups and acyl chains were synthesized. These lipids differ from each other with respect to the chemistry of the linker connecting the acyl chains to glutamide. Lipid **1** with the amide linker exhibited high transfection efficiency in four different cell lines,

dx.doi.org/10.1021/bc2002874 | *Bioconjugate Chem.* 2011, 22, 2244−2254

when compared to Lipid **2** with an ester linker. Among the popular colipids such as DOPE and cholesterol, both lipids exhibited higher transfection efficiency with cholesterol compared to DOPE. The binding of lipids to DNA in EtBr exclusion assay showed identical profiles, however, at charge ratios >1:1, Lipid **1** shows stronger displacement of EtBr. Similar charge ratio dependency was also observed in gel retardation assay with these lipids. Electron microscopy images of the lipoplexes prepared using Lipids **1** and **2** along with the colipids cholesterol and DOPE showed clearly that Lipid **1** lipoplexes have a defined morphology, whereas Lipid **2** aggregates were irregular and amorphous. Lack of defined liposomal structure of Lipid **2** vesicles was also confirmed by broad scattering profile in SAXS. It is apparent that the stronger binding and formation of defined stable complexes are important in the interaction of Lipid **1** with cells and eventually in their uptake. The higher uptake of the lipoplexes with Lipid **1**, as seen from confocal microscopy may consequently be responsible for observed higher transfection efficiency. Lipid **1** has also demonstrated efficient transfection in the presence of serum when tested in both CHO and HepG2 cells. The benefits of serum in transfection protocols have been reported.[29,30] Stability in serum suggests the potential of these lipids for DNA delivery *in vivo*.

Biophysical Basis for Higher Transfection Efficiency with Lipid 1. DNA binding being a prerequisite for achieving good transfection efficiency, it must be condensed prior to cell uptake. Cationic lipids bind electrostatically to the DNA.[3,30] This process results in condensation and protection of the DNA and leads to the formation of complexes that are particulate in nature.[3,31] DNA present in a particle is more efficiently taken up by the cell and endocytosed than free DNA. Characterization of lipoplexes at varying charge ratios revealed that transfection efficiency sharply increases with DNA condensation, change in zeta potential from negative to positive value, and observations of ordered lipoplexes in electron micrographs.[32] Although DNA was found to be condensed below optimal charge ratios, DNA was accessible to nucleases leading to decrease in transfection. Stability of the lipoplex is critical for protecting the DNA during transfection and also enhancing the uptake of the lipoplex by the cells.[32] Though binding of Lipid **2** with the DNA was comparable to Lipid **1**, the packing of the DNA into lipoplexes may be inefficient leading to particles that may be large and variable in size. Thus, Lipid **2**, a 12-carbon lipid, does not provide sufficient stability for the formation of liposomes; hence, its uptake by cells and subsequent transfection is poor. Though Lipid **1** has same chain length and headgroup as Lipid **2**, its melting temperature was nearly 40 °C higher. Melting temperature of lipids depends strongly on the length of the acyl chains and increases with the increase in chain lengths. Since Lipids **1** and **2** have identical chain lengths, the higher melting temperature may be due to additional interactions between the molecules. The stabilizing effect of the intermolecular hydrogen bond was observed between the headgroups in phosphatidylethanolamines (PE), which increases the melting temperature of PEs by nearly 20 °C compared to phosphatidylcholines of similar alkyl chain length.[33] Such intermolecular hydrogen bonding was observed in Gemini quaternary ammonium surfactants that contain an amide linker but not in ester-containing surfactants.[34] In addition, the data on polarization of DPH, an indicator of microviscosity of the membrane, suggests that both lipids possess similar microviscosity values, corroborating the observations that the higher melting temperature of Lipid **1** does not originate from the hydrophobic portion of the molecule. The addition of the slow compression rate of Lipid **1** monolayers compared to Lipid **2** also points to the fact that Lipid **1** monolayers experience additional intermolecular interactions. Since the head groups of both lipids are identical, the altered isotherm may originate intermolecular interactions. The amine linkers of Lipid **1** possibly form a hydrogen bond with carbonyl group of the adjacent lipid in a liposome, thus providing additional stability necessary for a stable lipoplex (Figure 10). In our opinion, this is the first report

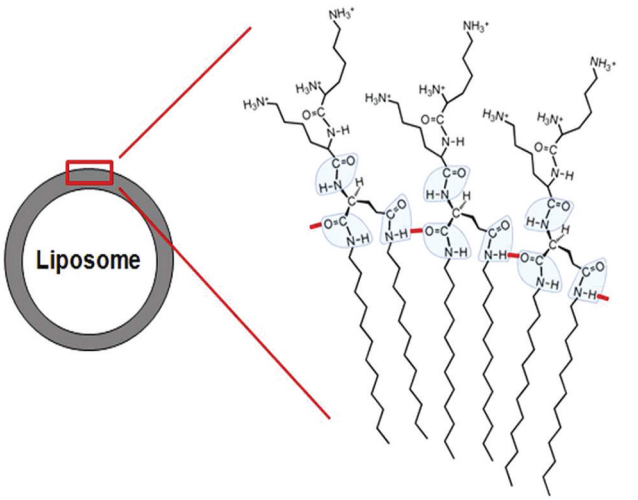

Figure 10. Intermolecular interactions of Lipid **1**. Model depicting stabilization of Lipid **1** through intermolecular interactions generated through hydrogen bonding.

of an approach to increase the stability and transfection of cationic liposomes by designing features favoring intermolecular hydrogen bonding.

Unsaturated lipids, predominantly oleic acid, containing cationic lipid formulations showed higher transfection efficiency than formulations with saturated lipids. Investigation of transfection efficiency with a given cationic lipid (DOTAP) along with phosphatidylethanolamine lipids with various acyl chains with different lengths indicated that unsaturated PEs are essential compared to saturated PEs for efficient transfection.[35] Hydrophobic moiety of cationic lipids strongly modulates their transfection activity. A study on the chain length variants of DOTAP suggests that DLTAP (*N*-[1-(2,3-dilauroyloxy)-propyl]-*N*,*N*,*N*-trimethylammonium methylsulfate) was least efficient in transfection.[36] In this context, the observation of higher transfection efficiency of Lipid **1**, despite having higher melting temperature, is interesting. It is observed that higher melting points of long acyl chain containing lipids do not mix with other membranes easily. Fusion between vesicles occurs readily above the phase transition temperature of the lipids. Below the phase transition temperature, the lipids are in crystalline phase and have restricted fluidity, essential for mixing of the membrane contents.[37] Within a cell, transfection processes involve membrane−membrane interactions between lipoplex and endosomal membrane and fusion.[38] Fusion is essential for dissociation of the cationic lipids from the DNA and release the DNA into the cytoplasm. Though Lipid **1** has higher melting temperature, its microviscocity as measured by DPH, is still in the range of 12-carbon lipids.

dx.doi.org/10.1021/bc2002874 | *Bioconjugate Chem.* 2011, 22, 2244−2254

Hence, the miscibility of Lipid **1** may not restrict fusion with other membranes. Amide linkers have been used in the design of cationic lipids and were found to be biodegradable and stable.[39] DOGS is a popular amide linker containing cationic lipid, where the amide linker is between the backbone and the headgroup.[40] A series of cationic lipids with amide and ester linkers to a pyridinium headgroup were synthesized. Amide linker containing lipids were found to be superior in transfection compared to the ester containing pyridinium lipids.[41] However, the amide containing lipids melt at slightly lower temperatures than the ester lipids. In another study, a series of detergents were synthesized with amide or ester linkers to amino acid head groups. The amide detergents bound to the oligonucleotides more efficiently than the ester containing detergents.[42] In Lipid **1**, the amide linker provides stability to the liposome and the lipoplex by forming an intermolecular hydrogen bond which did not seem to influence the membrane interactions crucial for transfection. Incorporating intermolecular interactions, such as hydrogen or ionic bonds, in cationic lipids offers yet another strategy to design efficient cationic lipids.

CONCLUSIONS

Stability of a lipoplex is important for achieving good transfection efficiencies. This is dependent on the nature of the cationic headgroup and DNA interactions and the hydrophobic volume of the lipid. The overview of lipid/DNA interactions and lipid properties of the two lipids, different in their linker chemistry, suggests that stable formation of liposomes with Lipid **1** was critical for superior transfection properties compared to Lipid **2**. Formulations made with Lipid **1** were stable in serum, thereby implying its utility for in vivo experimentation. Since the two lipids are identical in all aspects except for the linker, the stability of amide linker containing Lipid **1** is due to the presence of intermolecular hydrogen bonds leading to stable vesicles. This observation is supported by higher transition temperatures, TEM, SAXS, and monolayer studies. Incorporation of intermolecular interactions may be yet another way to increase the stability of the liposomes and thereby transfection.

ASSOCIATED CONTENT

Supporting Information

[Graphs depict thermal transitions of Lipids 1 and 2 using DPH, transfection efficiencies of Lipid analogues in comparison to Lipid 1 in CHO cells and transfection efficiency of Lipid 1 and 2 in HeLa cells. This material is available free of charge via the Internet at http://pubs.acs.org.

AUTHOR INFORMATION

Corresponding Author

*WP +91-40-27192514, Fax # +91-40-27160311, www.ccmb.res.in, E-mail: madhu@ccmb.res.in.

ACKNOWLEDGMENTS

This work was supported by JSPS-DST Bilateral Joint Project (# DST/INT/JSPS/Proj-38/2007) and a CSIR Network project (NWP0035). Advice of Drs. R. Nagaraj and B. Raman is gratefully acknowledged. We thank Nandini Rangaraj and Dr. Shoeb Ahmad for help with confocal microscopy and fluorescence anisotropy measurements, respectively. We thank Prasada Raju of Indian Institute of Chemical Technology, Hyderabad, for HR-ESI-MS analysis.

REFERENCES

(1) Chesnoy, S., and Huang, L. (2000) Structure and function of lipid-DNA complexes for gene delivery. *Annu. Rev. Biophys. Biomol. Struct. 29*, 27−47.

(2) Li, W., and Szoka, F. C. Jr. (2007) Lipid-based nanoparticles for nucleic acid delivery. *Pharm. Res. 24*, 438−49.

(3) Rao, N. M. (2010) Cationic lipid-mediated nucleic acid delivery: beyond being cationic. *Chem. Phy. Lipids 163*, 245−52.

(4) Nicolazzi, C., Garinot, M., Mignet, N., Scherman, D., and Bessodes, M. (2003) Cationic lipids for transfection. *Curr. Med. Chem. 10*, 1263−77.

(5) Audouy, S., and Hoekstra, D. (2001) Cationic lipid-mediated transfection in vitro and in vivo. *Mol. Membr. Biol. 18*, 129−43.

(6) Koynova, R., Wang., L., Tarahovsky, Y., and MacDonald, R. C. (2005) Lipid phase control of DNA delivery. *Bioconjugate Chem. 16*, 1335−9.

(7) Niculescu-Duvaz, D., Heyes, J., and Springer, C. J. (2003) Structure-activity relationship in cationic lipid mediated gene transfection. *Curr. Med. Chem. 10*, 1233−61.

(8) Barteau, B., Chèvre, R., Letrou-Bonneval, E., Labas, R., Lambert, O., and Pitard, B. (2008) Physicochemical parameters of non-viral vectors that govern transfection efficiency. *Curr. Gene Ther. 8*, 313−23.

(9) Montier, T., Benvegnu, T., Jaffrès, P. A., Yaouanc, J. J., and Lehn, P. (2008) Progress in cationic lipid-mediated gene transfection: a series of bio-inspired lipids as an example. *Curr. Gene Ther. 8*, 296−312.

(10) Tranchant, I., Thompson, B., Nicolazzi, C., Mignet, N., and Scherman, D. (2004) Physicochemical optimization of plasmid delivery by cationic lipids. *J. Gene Med. 6* (Suppl 1), S24−35.

(11) Gao, X., and Huang, L. (1991) A novel cationic liposome reagent for efficient transfection of mammalian cells. *Biochem. Biophys. Res. Commun. 179*, 280−5.

(12) Ren, T., Zhang, G., Liu, F., and Liu., D. (2000) Synthesis and evaluation of vitamin D-based cationic lipids for gene delivery in vitro. *Bioorg. Med. Chem. Lett. 10*, 891−4.

(13) Fichert, T., Regelin, A., and Massing, U. (2000) Synthesis and transfection properties of novel non-toxic monocationic lipids: Variation of lipid anchor, spacer and head group structure. *Bioorg. Med. Chem. Lett. 10*, 787−91.

(14) Floch, V., Loisel, S., Guenin, E., Hervé, A. C., Clement, J. C., Yaouanc, J. J., des Abbayes, H., and Férec, C. (2000) Cation substitution in cationic phosphonolipids: a new concept to improve transfection activity and decrease cellular toxicity. *J. Med. Chem. 43*, 4617−28.

(15) Heyes, J. A., Niculescu-Duvaz, D., Cooper, R. G., and Springer, C. J. (2002) Synthesis of novel cationic lipids: effect of structural modification on the efficiency of gene transfer. *J. Med. Chem. 45*, 99−114.

(16) Prasad, T, K., Rangaraj, N., and Rao, N, M. (2005) Quantitative aspects of endocytic activity in lipid-mediated transfections. *FEBS Lett. 579*, 2635−42.

(17) Hui, S. W., Langner, M., Zhao, Y. L., Ross, P., Hurley, E., and Chan, K. (1996) The role of helper lipids in cationic liposome-mediated gene transfer. *Biophys. J. 71*, 590−9.

(18) Simões, S., Slepushkin, V., Gaspar, R., de Lima, M. C., and Düzgüneş, N. (1998) Gene delivery by negatively charged ternary complexes of DNA, cationic liposomes and transferrin or fusigenic peptides. *Gene Ther. 5*, 955−64.

(19) Zuhorn, I. S., and Hoekstra, D. (2002) On the mechanism of cationic amphiphile-mediated transfection. To fuse or not to fuse: is that the question? *J. Membr. Biol. 189*, 167−79.

(20) Kumar, V. V., Pichon, C., Refregiers, M., Guerin, B., Midoux, P., and Chaudhuri, A. (2003) Single histidine residue in head-group region is sufficient to impart remarkable gene transfection properties to cationic lipids: evidence for histidine-mediated membrane fusion at acidic pH. *Gene Ther. 10*, 1206−15.

(21) Gopal, V., Prasad, T. K., Rao, N. M., Takafuji, M., Rahman, M. M., and Ihara, H. (2006) Synthesis and in vitro evaluation of glutamide-containing cationic lipids for gene delivery. *Bioconjugate Chem. 17*, 1530−6.

(22) Banerjee, R., Das, P. K., Srilakshmi, G. V., Chaudhuri, A., and Rao, N. M. (1999) Novel series of non-glycerol-based cationic transfection lipids for use in liposomal gene delivery. *J. Med. Chem. 42*, 4292−9.
(23) Kumar, V. V., Singh, R. S., and Chaudhuri, A. (2003) Cationic transfection lipids in gene therapy: successes, set-backs, challenges and promises. *Curr. Med. Chem. 10*, 1297−306.
(24) Rajesh, M., Sen, J., Srujan, M., Mukherjee, K., Sreedhar, B., and Chaudhuri, A. (2007) Dramatic influence of the orientation of linker between hydrophilic and hydrophobic lipid moiety in liposomal gene delivery. *J. Am. Chem. Soc. 129*, 11408−20.
(25) Ghosh, Y. K, Visweswariah, S. S., and Bhattacharya, S. (2002) Advantage of the ether linkage between the positive charge and the cholesteryl skeleton in cholesterol-based amphiphiles as vectors for gene delivery. *Bioconjugate Chem. 13*, 378−84.
(26) Legendre, J. Y., Trzeciak, A., Bohrmann, B., Deuschle, U., Kitas, E., and Supersaxo, A. (1997) Dioleoylmelittin as a novel serum-insensitive reagent for efficient transfection of mammalian cells. *Bioconjugate Chem. 8*, 57−63.
(27) Xavier, J., Singh, S, Dean, D. A., Rao, N. M., and Gopal, V. (2009) Designed multi-domain protein as a carrier of nucleic acids into cells. *J. Controlled Release 133*, 154−60.
(28) Hammersley, A. P., Svensson, S. O., Hanfland, M., Fitch, A. N., and Häusermann, D. (1996) Two-dimensional detector software: from real detector to idealised image or two-theta scan. *High Pressure Research 14*, 235−248.
(29) Simoes, S., Slepushkin, V., Pires, P., Gaspar, R., Pedroso de Lima, M. C., and Duzgunes, N. (2000) Human serum albumin enhances DNA transfection by lipoplexes and confers resistance to inhibition by serum. *Biochim. Biophys. Acta 1463*, 459−469.
(30) Tros de Ilarduya, C., Arangoa, M. A., and Duzgunes, N. (2003) Transferrin-lipoplexes with protamine condensed DNA for serum-resistant gene delivery. *Methods Enzymol. 373*, 342−356.
(31) Rao, N. M., and Gopal, V. (2006) Cell biological and biophysical aspects of lipid-mediated gene delivery. *Biosci. Rep. 26*, 301−24.
(32) Miller, A. D. The problem with cationic liposome/micelle-based non-viral vector systems for gene therapy. *Curr. Med. Chem. 10*, 1195-1211.
(33) Blume, A. (1983) Apparent molar heat capacities of phospholipids in aqueous dispersions: Effects of chain length and head group structure. *Biochemistry 22*, 5436−5442.
(34) Pisárčik, M., Polakovičová, M., Pupák, M., Devínsky, F., and Lacko, I. (2009) Biodegradable gemini surfactants. Correlation of area per surfactant molecule with surfactant structure. *J. Colloid Interface Sci. 329*, 153−159.
(35) Koynova, R., Tenchov, B., Wnag, L., and MacDonald, R. C. (2009) Hydrophobic moiety of cationic lipids strongly modulates their transfection activity. *Mol. Pharmaceutics 6*, 951−958.
(36) Regelin, A. E., Fankhaenel, S., Gürtesch, L., Prinz, C., von Kiedrowski, G., and Massing, U. (2000) Biophysical and lipofection studies of DOTAP analogs. *Biochim. Biophys. Acta 1464*, 151−164.
(37) Ma, B., Zhang, S., Jiang, H., Zhao, B., and Lv, H. (2007) Lipoplex morphologies and their influences on transfection efficiency in gene delivery. *J. Controlled Release 123*, 184−94.
(38) Friend, D. S., Papahadjopoulos, D., and Debs, R. J. (1996) Endocytosis and intracellular processing accompanying transfection mediated by cationic liposomes. *Biochim. Biophys. Acta 1278*, 41−50.
(39) Niculescu-Duvaz, D., Heyes, J., and Springer, C. J. (2003) Structure-activity relationship in cationic lipid mediated gene transfection. *Curr. Med. Chem. 10*, 1233−61.
(40) Behr, J. P., Demeneix, B., Loeffler, J. P., and Perez-Mutul, J. (1989) Efficient gene transfer into mammalian primary endocrine cells with lipopolyamine-coated DNA. *Proc. Natl. Acad. Sci. U. S. A. 86*, 6982−6.
(41) Zhu, L., Lu, Y., Miller, D. D., and Mahato, R. I. (2008) Structural and formulation factors influencing pyridinium lipid-based gene transfer. *Bioconjugate Chem. 19*, 2499−2512.
(42) Santhiya, D., Dias, R. S., Shome, A., Das, P. K., Miguel, M. G., Lindman, B, and Maiti, S. (2009) Role of linker groups between hydrophilic and hydrophobic moieties of cationic surfactants on oligonucleotide-surfactant interactions. *Langmuir 25*, 13770−13775.